

1
2 Assessment of a Physical-Biogeochemical Coupled Model System for
3 Operational Service in the Baltic Sea
4
5
6
7
8

9 Zhenwen Wan^{1*}, Jun She¹, Marie Maar², Lars Jonasson¹, Jesper Baasch-Larsen³
10
11

12 1. Centre for Ocean and Ice, Danish Meteorological Institute, Lyngbyvej 100, DK-2100
13 Copenhagen, Denmark

14 2. National Environmental Research Institute, Aarhus University, Department of Marine Ecology,
15 Frederiksborgvej 399, PO box 358, DK-4000 Roskilde, Denmark

16 3. Danish Defence Center for Operational Oceanography, Overgaden Oven Vandet 62B, DK-1023
17 Copenhagen K, Denmark
18
19
20

21 *Corresponding author: zw@dmi.dk, phone: 0045 3915 7284, fax: 0045 3915 7300
22
23
24

25 Key words: ecosystem model, ecological model, biogeochemical model, Baltic Sea, model
26 assessment, model validation, operational oceanography
27

28 Abstract

29 Thanks to the abundant observation data, we are able to deploy the traditional point-to-point
30 comparison and statistical measures in combination with a comprehensive model validation scheme
31 to assess the skills of the biogeochemical model ERGOM in providing an operational service for the
32 Baltic Sea. The model assessment concludes that the operational products can resolve the main
33 observed seasonal features for phytoplankton biomass, dissolved inorganic nitrogen, dissolved
34 inorganic phosphorus and dissolved oxygen in euphotic layers, as well as their vertical profiles.
35 This assessment reflects that the model errors of the operational system at the current stage are
36 mainly caused by insufficient light penetration, excessive organic particle export downward,
37 insufficient regional adaptation and some of improper initialization. This study highlights the
38 importance of applying multiple schemes in order to assess model skills rigidly and identify main
39 causes for major model errors.

40

41

42 1. Introduction

43 Assessment of an operational model is different from validation of a model targeted at a specific
44 research task. An operational model should serve broader interests than a research model generally
45 does, since the users of the model results can be interested in various subdomains and processes.
46 This is especially true during the early development phase of an operational model to supply
47 biogeochemical information service. During the preliminary phase, there are no specific user needs,
48 simply because user groups have not been well developed yet. Of course, there are general concerns
49 in ecological operational oceanography, e.g. eutrophication, harmful algae blooms and oxygen
50 depletion. Therefore, an operational model should produce sensible results in the entire model
51 domain for all targeted state variables. In fact, the development of ocean models are endless
52 practices where developers always do their best to work towards moving targets. As a goal of this
53 stage, the model is aiming at reproducing the main observed seasonal features for phytoplankton
54 biomass, nutrients concentration and dissolved oxygen concentration in euphotic layers.

55 Various ecosystem models have been developed for the Baltic Sea (Neumann, 2000; Edelvang et
56 al., 2005; Savchuk et al., 2008; Eilola et al., 2009). The biogeochemical model ERGOM developed
57 by Neumann (2000) and Neumann et al. (2002) has been applied in a number of investigations of
58 the Baltic Sea ecosystem. The model inherited the advances of previous ecological models
59 developed for the Baltic Sea (Stigebrandt and Wulff, 1987; Fennel, 1995; Fennel and Neumann,
60 1996) and has been further developed. Fennel and Neumann (2003) introduced stage-structured
61 copepod models in order to replace the bulk description of zooplankton and improve the link to
62 higher trophic levels. In the study on eutrophication and shifts in nitrogen fixation, Neumann and
63 Schernewski (2008) introduced iron-phosphate-complex in combination with Dissolved Inorganic
64 Phosphorus (DIP) in order to simulate the mineralization of detritus in the sediment. Kuznetsov et
65 al. (2008) added seven state variables so as to simulate C, N, P cycling separately. Maar et al.
66 (2011) added silicate as one more state variable so as to be able to model the ecosystem in the entire

67 salinity gradient region covering the Baltic Sea and the North Sea. Other examples of ERGOM
68 application studies include the inter-annual variability in cyanobacteria blooms (Janssen et al.,
69 2004), the assessment of two nutrient abatement strategies (Neumann and Schernewski, 2005), and
70 the fate of river-borne nitrogen (Neumann, 2007).

71 As one part of the EU projects ECOOP (<http://www.ecoop.eu>) and MyOcean
72 (<http://www.myocean.eu.org>), the ecosystem model ERGOM (Neumann, 2000; Neumann et al.,
73 2002) is coupled with the circulation model HBM (<https://hbmsvn.dmi.dk/>) (Berg and Poulsen,
74 2012) for providing GMES (Global Monitoring of Environment and Security) Marine Service in the
75 Baltic Sea. This paper presents an assessment of the operational model system with focus on its
76 biogeochemical service, through comparing model results and observations comprehensively.

77 2. Models, data and methods

78 2.1 Physical model

79 The physical model is the HIROMB-BOOS ocean circulation model (HBM) (Berg and Poulsen,
80 2012). The core of the physical model, the circulation model, is based on the primitive geophysical
81 fluid dynamics equations for the conservations of volume, momentum, salt and heat. The circulation
82 model has been coupled to a Hibler-type sea ice model. The wind, air pressure, air temperature,
83 humidity, evaporation/precipitation and cloud cover are taken into account in the parameterizations
84 of surface boundary conditions. Water levels of tides and surges and monthly climatology of
85 temperature and salinity are imposed as outer lateral boundary conditions. River runoff is included
86 as an inner lateral condition. The model setup fully covers both the Baltic Sea and the North Sea
87 with four two-way nested subdomains (Table 1). Our targeted area is the Baltic Sea (Fig. 1)

88 Table 1. Model grids

Subdomains	Longitude	Latitude	Lon.Res	Lat.Res	Lay.
------------	-----------	----------	---------	---------	------

North Sea	4°07'30"W-11°57'30"E	48°31'30"-65°52'30"N	5'	3'	50
Danish Straits	9°20'25"-14°49'35"E	53°35'15"-57°35'45"N	50"	30"	75
Wadden Sea	6°10'50"-10°29'10"E	53°13'30"-55°41'30"N	1'40"	1'	24
Baltic Sea	14°37'30"-30°17'30"E	53°31'30"-65°52'30"N	5'	3'	109

89 Abbreviations: Lat.Res for latitude resolution, Lon.Res for longitude resolution, Lay. for number of
90 layers.

91 Location for Fig. 1

92 The products by the operational weather model High Resolution Limited Area Model of the Danish
93 Meteorological Institute are used to provide atmospheric forcing drivers for the physical model (She
94 et al., 2007a). The daily river runoffs are provided by the operational hydrological model HBV run
95 by the Swedish Meteorological Hydrological Institute (Bergström, 1976 and 1992) in combination
96 with observations from the German Bundesamt für Seeschifffahrt und Hydrographie and
97 climatology. The previous versions of HBM were validated by She et al. (2007a, b). The current
98 version was validated in the Scientific Calibration Report V2 for WP6
99 (<http://www.myocean.eu.org/>).

100 2.2 Ecosystem model

101 The applied version of ERGOM is close to the original version by Neumann et al. (2002). ERGOM
102 originally adopted Redfield ratio for the phytoplankton stoichiometry. Wan et al. (2011)
103 documented that a non-Redfield ratio is more suitable in the Baltic Sea than the Redfield ratio.
104 Moreover, Wan et al. (2012) demonstrated that a spatially variable N/P ratio is more close to the
105 real phytoplankton stoichiometry in the Baltic Sea than a fixed non-Redfield ratio does. In the
106 current study, the model setup and configuration are the same as in the MyOcean Scientific
107 Calibration Report V2 for WP6, but the source code is upgraded to implement the spatially variable
108 N/P ratio (Wan et al., 2012).

109 Initial fields for ammonia, nitrate, DIP and Dissolved Oxygen (DO) are set through merging the
110 data from the World Ocean Atlas 2001 (WOA01, Conkright et al., 2002) and the data from the
111 International Council for the Exploration of the Sea (ICES) (<http://www.ices.dk/indexfla.asp>).
112 Initial fields for the biological state variables have been adjusted through repetitive runs. The open
113 boundary conditions for nitrate, DIP and DO are interpolated from the climatology of WOA01 data
114 while the remaining state variables are set to zero. The bioloadings are from the same data sources
115 for river runoffs mentioned above. The atmospheric nutrient depositions are based on Langner et al.
116 (2009) and Eilola et al. (2009).

117 2.3 The comprehensive validation scheme

118 The comprehensive validation scheme makes use of all available in-situ data in order to reflect the
119 model skill overall, rather than only at selected stations or over a part of the spatio-temporal
120 domain. This scheme compares model results with observations along the specified dimension (e.g.
121 temporal evolution, vertical profile or horizontal distribution). For technical details, refer to Wan et
122 al. (2011). In this study, the 4-dimensional spatiotemporal grid to delimit data representation has a
123 horizontal resolution of 0.5°x0.5°, a vertical resolution of 4 m and a temporal resolution of 15 days.

124 2.4 Statistical measures

125 To assess the model skills we use the following statistical measures: coefficient of determination
126 (R^2), i.e. square of correlation coefficient, Model Efficiency (ME) (Nash and Sutcliffe, 1970), Cost
127 Function (CF) (OSPAR Commission, 1998) and Percentage of Bias (PB) (Allen et al., 2007). ME is
128 a measure of the ratio of the model error to the data variability,

$$129 \quad ME = 1 - \frac{\sum (D - M)^2}{\sum (D - \bar{D})^2}, \quad (1)$$

130 where D is the data, M is the corresponding model value, while the overbar denotes an averaging

131 operation. ME is cited as a performance indicator: >0.65 excellent, 0.65-0.5 very good, 0.5-0.2
132 good, <0.2 poor (Maréchal, 2004). CF is a measure of the “goodness of fit” between model and
133 data,

$$134 \quad CF = \frac{\sum |M - D|}{n\sigma_D}, \quad (2)$$

135 where σ_D is the standard deviation of data and n is the number of samples in the dataset. CF is
136 cited as a performance indicator: <1 very good, 1-2 good, 2-3 reasonable, >3 poor (Radach and
137 Moll, 2006). |PB| is cited as a performance indicator: <10 excellent, 10-20 very good, 20-40 good,
138 >40 poor (Maréchal, 2004) and PB is given,

$$139 \quad PB = \frac{\sum (D - M)}{\sum D} * 100 \quad (3)$$

140 2.5 Observations

141 The observations used for model assessment are downloaded from ICES database. We have used
142 the following observation types: temperature, salinity, chlorophyll (Chl) a , Dissolved Inorganic
143 Nitrogen (DIN = ammonia + nitrate only), dissolved inorganic phosphorous and DO. The data
144 coverage ranges $10^\circ \sim 30^\circ E$ and $54^\circ \sim 66^\circ N$ (Fig. 1) and from January 1, 2007 to December 31, 2008.
145 The total record numbers for temperature, salinity, Chl a , DIN, DIP and DO are listed in Table 3.
146 The ICES database is searched for monthly based time-series records. It ends up with 18 stations
147 which have monthly based time-series records for almost all of the targeted state variables during
148 2007 and 2008. The station locations are shown in Fig. 1.

149 2.6 Simulation

150 The simulation is the same as the inter-comparison experiment described in the Scientific
151 Calibration Report V2 for WP6 of the MyOcean project, i.e. a model hindcast for years of 2007 and

152 2008. The only difference to that inter-comparison experiment is using the upgraded source code
 153 with a spatially variable N/P ratio (Wan et al., 2012).

154 3. Results

155 Although ERGOM includes nine state variables, we present the model-observation comparison for
 156 only DIN, DIP, Chl *a* and DO, in consideration of the availability of observations. Temperature and
 157 salinity of the model results are also compared with observations in order to supply information on
 158 the skills of the circulation model. We examine the temporal dynamics in surface and bottom layers
 159 at 18 stations (Fig.s 2-12), the vertical profile at Station I in the Gotland deep (Fig. 13) and the bias
 160 distribution along different dimensions (Fig.s 14-16). The surface/global statistical measures are
 161 listed in Tables 2 and 3, whose performance scores are listed in Table 4.

162 Table 2. Statistical measures of model-observation comparison in the surface layer

	NS	Mean ^o	Mean ^m	PB	R ²	ME	CF
temperature	2077	9.8	9.7	-1.1	0.94	0.93	0.07
Salinity	2008	9.3	9.2	-1.1	0.96	0.96	0.05
DIN	1548	3.6	1.5	-58	0.10	0.04	19.0
DIP	1551	0.34	0.33	-4.7	0.35	0.33	1.3
Chl <i>a</i>	1291	3.5	3.0	-14	0.06	0.03	6.9
DO	1814	352	337	-4.0	0.34	0.21	1.2

163 Abbreviations: NS for number of samplers, Mean^o for mean value of observations, Mean^m for mean
 164 value of model results, PB for percentage of bias, R² for square of correlation coefficient, i.e.
 165 coefficient of determination, ME for model efficiency, CF for cost function.

166

167 Table 3 Statistical measures of model-observation comparison overall

	NS	Mean ^o	Mean ^m	PB	R ²	ME	CF
temperature	16534	7.8	7.9	1.2	0.89	0.89	0.11
salinity	16208	11	11	-2.2	0.98	0.98	0.02
DIN	10517	3.1	4.6	26	0.07	-0.18	2.24
DIP	10549	0.90	1.1	-2.2	0.87	0.86	0.22
Chl <i>a</i>	5644	2.3	2.7	-14	0.15	0.11	3.09
DO	14070	276	290	4.9	0.80	0.77	0.36

168 Abbreviations same as in Table 2.

169 Table 4 Performance scores

	Surface layer			All layers		
	PB	ME	CF	PB	ME	CF
DIN	Poor	Poor	Poor	Good	Poor	Reasonable
DIP	Excellent	Good	Very good	Excellent	Excellent	Very good
Chl <i>a</i>	Very good	Poor	Poor	Very good	Poor	Poor
DO	Excellent	Good	Very good	Excellent	Excellent	Very good

170 Scores are accorded to Nash and Sutcliffe (1970), OSPAR Commission (1998) and Allen et al.
171 (2007).

172 3.1 Temperature

173 In the surface layer, the model results fit observations very well at all the 18 stations in terms of
174 seasonal variability (Fig. 2). In details, model matches observation best in the winter months but
175 with more bias in the summer months, which can be up to 2 °C off. Northeastern Baltic sea coastal
176 stations (M, O, R) have larger model errors than others. In statistics using all model-observation
177 pairs in surface layer (far beyond 18 stations), PB is -1.1 only, R² is up to 0.94, ME is up to 0.93,
178 and CF is 0.07 (Table 2). It means that the performance scores are either “excellent” or “very good”
179 in the surface layer.

180 In the bottom layer, the seasonal cycle is less visible at water depth deeper than 50 m. The model
181 catches the observed seasonal pattern for the shallow stations in Kattegat, Western Baltic Sea,
182 Bothnian Sea and Bothnian Bay (C, D, N, P, Q and R) and the deep stations in Central and North
183 Baltic Proper (F-K), but are rather off for stations A, E, L (Fig. 3). The temporal evolution of
184 vertical profiles of the model (Fig. 13a) matches well that of observations in general (Fig. 13g).
185 There are however some minor errors. For example, the model temperature at depth 90-120 m is
186 persistently higher than observations, and there exists downward temperature gradient in November
187 and December above 40 m in model results but not in observations which indicates that the model
188 has less vertical mixing. The spatial mean of observations is caught well by the corresponding mean
189 of model results (Fig. 14a). The mean of observations at one depth plane is also well reproduced by
190 the corresponding model results (Fig. 15a), but the model errors are larger in layers below 100 m
191 than above, up to 0.5 °C. The percentage bias of model to observation is mostly smaller than $\pm 10\%$
192 (Fig. 16a). The global statistical measures PB, R^2 , ME and CF are 1.2, 0.89, 0.89 and 0.11,
193 respectively (Table 3). It means that the performance scores are also either “excellent” or “very
194 good” in the bottom layer.

195 Location for Fig. 2

196 Location for Fig. 3

197

198 3.2 Salinity

199 In the surface layer, the model results reproduce the observed seasonal variability in south of 59°N,
200 i.e. stations A-K, where salinity is higher than 6.0 psu (Fig. 4). No salinity observations are
201 available at stations L and M. At stations N-R , the mean values of model results are close to those
202 of observations, but the model cannot reproduce the fine seasonal dynamics which is mostly smaller
203 than 1.0 psu. The surface statistical measures PB, R^2 , ME and CF are -1.1, 0.96, 0.96 and 0.05,

204 respectively (Table 2).

205 In the bottom layer, seasonal cycle is not visible (Fig. 5). The fit between model results and
206 observations is quite similar as in surface layer (Fig. 5). The temporal profile of model results (Fig.
207 13b) matches that of observations in general (Fig. 13h). The observed halocline depth is around 60
208 m, while the modeled one varies between 40 m and 80 m. The spatial mean of the salinity
209 observations is caught perfectly by the model (Fig. 14d). The mean of the observations at one depth
210 plane is also well reproduced (Fig. 15d). Regarding the spatial distribution of the model errors, the
211 percentage bias of the model to observation is mostly smaller than $\pm 5\%$ (Fig. 16 d). The model
212 generally has positive biases in coastal regions, but negative biases in offshore regions. The model
213 bias can be larger than $\pm 10\%$ in the Bothnian Bay. The global statistical measures PB, R^2 , ME and
214 CF are -2.2, 0.98, 0.98 and 0.02, respectively (Table 3).

215 Location for Fig. 4

216 Location for Fig. 5

217

218 3.3 DIN

219 In the surface layer, the model results at all the 18 stations reproduce the observed seasonal
220 variability, high values during winter and low values during summer (Fig. 6). For winter nutrients,
221 the model underestimates the surface DIN in the western Baltic Sea (stations A-D) and Gulf of
222 Finland (stations L-O) but with a fine match in the central Baltic Sea (stations E-K), Bothnian Sea
223 and Bothnian Bay (stations P-R). Notably, the underestimation of DIN decreases from Eastern
224 Skaggerrek to Kategatte and Arkona Basin (stations A-D). The timing of abrupt DIN consumption in
225 model results is consistent with that in observations at the deep water stations G-K, but later than
226 that of observations in coastal stations A-F, M-P and R. The surface statistical measures PB, R^2 , ME

227 and CF are -58, 0.10, 0.04 and 19, respectively (Table 2). The performance indicators, however,
228 show the model quality of surface DIN quality is “poor” (Table 4) although as shown above, the
229 modeled surface DIN does reproduce many important measured features at the 18 stations.

230 In the bottom layer, seasonal pattern of DIN varies between stations. Clear pattern is found in the
231 stations north of 59N (L-R), with high values in winter and low values in summer. No clear
232 seasonal change patterns can be identified in stations A-K. The model results are close to the
233 observed seasonal variations at the shallow water stations C, D, M, O, P and Q, and reproduce the
234 basic seasonal pattern at stations B, L, N and R, but are rather off at deep stations A and F-K (Fig.
235 7). It is noted that the overestimation of the bottom DIN is only found in the central Baltic Sea
236 (stations G-K). At the shallower stations, the model estimates mean DIN well except for a
237 underestimation of the winter DIN in Gulf of Finland (stations L-N). The temporal evolution of the
238 vertical profile at station I shows that the model can reflect the observed seasonal variations only in
239 the upper 20 m. Model results for DIN (Fig. 13c) are much higher than observations in layers 80 m
240 below (Fig. 13i). The seasonal variation is less than that of observations (Fig. 14e). The model
241 generally underpredicts DIN above 30 m, but overpredicts below 60 m (Fig. 15e). The model bias
242 has a clear horizontal pattern (Fig. 16e). Negative model bias mainly appears in the Danish Straits,
243 the Polish coasts, the Gulf of Finland and the Finland coasts, while large positive model bias
244 appears in the western Baltic proper and the western Bothnian Sea. The global statistical measures
245 PB, R^2 , ME and CF are 26, 0.07, -0.18 and 2.24, respectively (Table 3), which is “poor” for ME,
246 “reasonable” for CF and “good” for PB (Table 4).

247 Location for Fig. 6

248 Location for Fig. 7

249

250 3.5 DIP

251 In the surface layer, the model reproduces the basic seasonal variation pattern, with high values
252 during winter and low values during summer at all the 18 stations (Fig. 8). The model results match
253 observations at offshore stations E-K, and can only follow the basic seasonal pattern but not resolve
254 the detailed variations at the coastal stations M-P. The model errors of the surface DIP are similar to
255 that of the surface DIN. The winter DIP peak values are underestimated in coastal stations A-D and
256 N-O. The surface statistical measures PB, R^2 , ME and CF are -4.7, 0.35, 0.33 and 1.3, respectively
257 (Table 2), which implies that the model quality is “good” to “excellent” for the surface DIP in terms
258 of the performance indicators in Table 4.

259 In the bottom layer, the model results are close to observations and can reproduce the observed
260 seasonal variability at most of stations, except coastal stations A, J, L and R (Fig. 9). The temporal
261 evolution of vertical profile shows that the model can reproduce the observed seasonal variability in
262 upper 20 m (Fig. 13d, j) and the model results are close to observations in layers 80 m below. The
263 seasonal pattern of model results mostly follows that of observations, except that the model
264 underpredicts DIP during winter (Fig. 14c). The model results match well the observations in
265 vertical profiles (Fig. 15c). The horizontal distribution of model bias is featured with large positive
266 values in the Bothnian Sea and the Bothnian Bay (Fig. 16c). The highest PB is up to 100 and even
267 higher. The global statistical measures PB, R^2 , ME and CF are -2.2, 0.87, 0.86 and 0.22,
268 respectively (Table 3). This indicates that overall performance of the model in simulating DIP is
269 “excellent” (Table 4).

270 Location for Fig. 8

271 Location for Fig. 9

272

273 3.6 Chl *a*

274 In the surface layer, the model reproduces the basic seasonal variation pattern with 2 or 3 bloom
275 peaks during April to October and a recession during November to February (Fig. 10). The model's
276 bloom peak values are generally larger than 3 mg m^{-3} and the recession values are smaller than 1 mg
277 m^{-3} , which are close to those of observations. The surface statistical measures PB, R^2 , ME and CF
278 are -14, 0.06, 0.03 and 6.9, respectively (Table 2), which gives a "good" performance in terms of
279 PB and "poor" in ME and CF (Table 4).

280 The model results show that Chl *a* mostly appear in the upper layer 30 m above (Fig. 13e), in
281 agreement with observations (Fig. 13k). The temporal evolution of the vertical profile of
282 observations is quite complex, which the model fails to reproduce. The spatial means show that the
283 general seasonal evolution of model results is close to that of observations, but the model
284 underpredicts spring bloom peak, especially in year 2008 (Fig. 14b). The overall vertical profile of
285 model results is quite consistent with that of observations (Fig. 15b). The model results have
286 positive biases in the Danish Straits, the Gulf of Finland and the Bothnian Bay, and negative bias in
287 the Baltic proper (Fig. 16b). As Chl *a* appears mainly in the upper layers 20 m above, the global
288 statistical measures are close to the surface statistical measures. The global statistical measures PB,
289 R^2 , ME and CF are -14, 0.15, 0.11 and 3.09, respectively (Table 3), which means "very good" in
290 terms of PB, but "poor" in ME and CF.

291 Location for Fig. 10

292 3.7 DO

293 In the surface layer, model results are generally consistent with observations at all the 18 stations in
294 terms of seasonal variability (Fig. 11). The consistency seems to decrease with salinity. The model
295 has one month advance of the timing of the seasonal maxima during spring. The surface statistical
296 measures PB, R^2 , ME and CF are -4.0, 0.34, 0.21 and 1.2, respectively (Table 2), with performance
297 scores ranging from "very good" to "excellent" (Table 4).

298 In the bottom layer, the model reproduces seasonal variations at shallow water stations, but is rather
299 off at the deep water stations E-K (Fig. 12). The temporal evolution of the vertical profile shows
300 that the model (Fig. 13f) can reproduce the seasonal variation of observations (Fig. 13l) in the upper
301 60 m, but diverges in layers 60-120 m. The observed minima within euphotic layers appear
302 subsurface during summer, but the corresponding modeled minima appear at the surface. The
303 modeled summer values (June-October) are generally higher than observations (Fig. 14f). The
304 general vertical profile of model results is close to that of observations, but the biases increase
305 downward below 60 m (Fig 15f). The model errors are mostly smaller than $\pm 20\%$ (Fig. 16f).
306 Relative large model errors exist in the western Baltic proper and the western Bothnian Sea. The
307 global statistical measures PB, R^2 , ME and CF are 4.9, 0.80, 0.77 and 0.36, respectively (Table 3),
308 with performance scores ranging from “very good” to “excellent” (Table 4).

309 Location for Fig. 11

310 Location for Fig. 12

311 Location for Fig. 13

312 Location for Fig. 14

313 Location for Fig. 15

314 Location for Fig. 16

315

316 4. Discussions

317 4.1 Model validity

318 The comprehensive comparison presented above includes the model-observation pairs in the order

319 of 10^4 for almost every targeted state variable, thanks to the relatively abundant observation
320 network in the Baltic Sea. Though the model-observation comparison is comprehensive, it is not
321 obvious which aspects of model results are valid as the products of operational oceanography.
322 Literally, model validation is a general phrase which might generate confusions sometimes and
323 needs clarifications specifically (Rykiel, 1996; Radach and Moll, 2006). There are no written
324 criteria to judge whether a model is valid for operational oceanography. While we are developing
325 and improving our operational model system, we follow two criteria: that the quantitative model
326 skills should be among the right order of this type of models, and that the model should be able to
327 reproduce major observed features for interested scales.

328 As values of ecological parameters can differ a lot across systems, various statistical measures have
329 been adopted in assessing model skills in previous studies. The statistical measures CF, ME and PB
330 are applied in the ecological model validation studies nearby the Baltic Sea (Radach and Moll,
331 2006; Allen et al., 2007; Neumann and Schernewski, 2008; Lewis and Allen, 2009). According to
332 these three statistical criteria (Maréchal, 2004; Radach and Moll, 2006) and the results (Table 3),
333 the model skills for temperature, salinity, DIP and DO are scored either “excellent” or “very good”.
334 The model skill for Chl *a* is only scored “very good” of PB criterion, but “poor” according to both
335 CF and ME criteria. The model skill for DIN is scored “good” of PB criterion, “reasonable” of CF
336 criterion, but “poor” according to ME criterion. Although same “scores” do not always mean same
337 level of model performances, the statistical measures provide a possibility to inter-compare skills
338 across models applied in different regions. In comparison with other models in the Baltic Sea and
339 nearby regions, the overall skills of this model system are at the same level of this type of models
340 (Edelvang et al., 2005; Lacroix et al., 2007; Lewis and Allen, 2009, Almroth and Skogen 2010).

341 4.1.1 Model validity of seasonal variability in surface

342 Observations show spring blooms start in March and last to late April or early May. The system is
343 featured with abrupt nutrient consumption for both DIN and DIP and a similar abrupt increase of

344 phytoplankton biomass. The model captures these features (Fig. 6, 8, 10), although there is some
345 timing delay at stations outside of the Baltic proper. After spring blooms until late October or early
346 November, surface DIN remains depleted at most of stations, surface DIP however is only depleted
347 for a rather short duration at the shallow water stations, but continuously decreases and then
348 gradually recovers from July at the deep water stations E-K. In autumn, the system is featured with
349 abrupt nutrient recovery by wind mixing and autumn blooms of phytoplankton. During winter,
350 nutrient concentrations remain high and phytoplankton biomass remains low. These features are
351 mostly captured by the model (Fig. 6, 8, 10).

352 The model-observation biases of Chl a in surface layer seems unusually high in summer at Stations
353 O and P, meanwhile the observed Chl a is unusually low (Fig. 10). The satellite detected Chl a
354 (<http://marcoast.dmi.dk/chlorophyll.php>) is used as another reference. The modeled Chl a is
355 compared with the satellite detected Chl a (Fig. 17). Both the modeled and satellite detected Chl a
356 are mostly higher 4 mg m^{-3} in June and July at those two stations, but the observational Chl a is
357 lower than 2 mg m^{-3} , which is unusual in summer. We think the observations at those two stations
358 might be problematic. The additional comparison provides also a reference for stations where in-
359 situ observations are missed, e.g. at Station Q, and Station E in 2007. All in all, the modeled Chl a is
360 quite consistent with the satellite detected Chl a, except for winter months. In winter, the satellite
361 detected Chl a is generally poor and much discrepancy with observations.

362 Location for Fig. 17.

363 4.1.2 Model validity of vertical profile

364 The model generally reproduces the observed vertical profiles except poorly for DIN (Fig. 15). The
365 temporal evolution of vertical profiles at the Gotland Deep station I shows that the model's vertical
366 profiles are close to the observed ones, although there is a lot of fine difference (Fig. 13). For
367 example, the maximum vertical gradient appears at depth of 60 m for observations (Fig. 13b, c, d,

368 f), but the corresponding model position is at depth of 80 m (Fig. 13h, i, j, l). It means the vertical
369 profiles of model at a specific station are not always consistent with observations, however, the
370 overall pattern of vertical profiles are generally good. We think that the model errors at different
371 horizontal locations probably cancel out greatly.

372 4.2 Model errors and likely causes

373 4.2.1 Insufficient light penetration

374 The model underestimates the amplitudes of seasonal variations for Chl *a*, DIN, DIP and DO (Fig.
375 14b, c, e, f). In details, the model underestimates the seasonal maxima for Chl *a*, DIN, DIP, but
376 overestimates the seasonal minimum for DO. We think the insufficient light penetration is the main
377 cause. The observed DIN is depleted down to 40-60 m (Fig. 13c), but the model results show DIN
378 depletion is only down to 30 m and the duration of DIN depletion is shorter. The insufficient light
379 penetration leads to underestimation of nutrient uptake and phytoplankton biomass. It means the
380 primary production is underestimated, thus the maximum DO concentration during spring blooms is
381 underpredicted (Fig. 11).

382 4.2.2 Bottom layer vulnerability in deep water areas

383 The model results reflect a model vulnerability in bottom layer in deep water areas, i.e. in the
384 Gotland deep. The first, the modeled bottom salinity are continuously decreasing at Stations I and J,
385 but there are no clear decreasing trends in observations (Fig. 5, i, j). The second, the observed
386 bottom DIN at the Gotland deep (Station I) has an obvious increasing trend from May of 2007 to
387 July of 2008, however, the corresponding model results show a decreasing trend (Fig. 7, i). The
388 likewise model-observation discrepancy occurs as to DIP (Fig. 9, i). The third, the observed bottom
389 DO shows a decreasing trend, however, the corresponding model results show an increasing trend
390 (Fig. 12, i). The negative DO gets larger and larger, meaning hydrogen sulphide was taking place.

391 The main cause for this model vulnerability is due to the improper vertical grid. Although the model
392 has 109 vertical layers from the Baltic Sea (Table 1), they are arranged: 2 m for the surface layer, 1 m
393 for each of the following 98 layers, and 3 m, 6 m, 8 m, 16 m, 25 m for the 100-104th layer
394 respectively, and 50 m for each of the rest 5 layers. The thickness of bottom layer at both Stations I
395 and J are 50 m. At first, the too thick bottom layer introduced errors in the initialization, as we see
396 the initial bottom DO was set positive due to grid interpolation (Fig. 12, i). Actually, the initial
397 bottom nitrate was also wrongly set much higher than observation for same reason (not presented).
398 The model results in the bottom layer at Station I reflect that the dead organic detritus was
399 remineralized first through consuming the positive DO and then through oxidizing the wrongly
400 initialized high nitrate. In fact, the real remineralization was occurring through oxidizing sulphide,
401 as the negative DO increased. The second, the too thick bottom layer diluted the effects of water-
402 sediment flux on the bottom water. That's why the modeled dynamics in the bottom layer is slow,
403 not comparable to the observed dynamics. The third, too thick bottom might not accurately
404 reproduce the hydrodynamics, as we see the model-observation discrepancy for salinity (Fig. 5, i, j).
405 Inaccurate hydrodynamics could also exacerbate the model biases.

406 If the initialization errors are negligible and the real variations are not dramatic, the model can
407 follow observations in the bottom layer in deep water areas, as we see at Stations J and K (Fig.s 7,
408 9, 12). It means the model does not include fundamental errors. This supports the speculation that
409 the model vulnerability failed to recaptured the observed biogeochemical dynamics at the Gotland
410 deep was mainly caused by the improperly coarse vertical grid. On the other hand, there might exist
411 another possibility: the remineralization rate under anoxic condition might also be slower than the
412 reality.

413 4.2.3 Insufficient regional adaptation

414 Although the horizontally variable N/P ratio improves the model adaptation for different regions
415 (Wan et al., 2012), the model shows better performance in offshore regions than in coastal regions,

416 and better in the Baltic proper than outside (Fig. 16). The model shows the best performance for the
417 deep water stations (F-K). This might be caused by the parameter values being tuned for the Baltic
418 proper (Neumann, 2000; Neumann et al., 2002). The model's regional adaptation can be further
419 improved by allowing more parameters to vary regionally and refining the boundary inputs, like
420 river loadings. Modeled spring blooms at stations outside of the Baltic proper occur later than
421 observed. Suspended particles are reported influential for the timing of spring blooms (Tian et al.,
422 2010).

423 4.2.4 Uncertainties in forcing and initialization

424 One of the major model errors in DIN and DIP occur in coastal regions influenced by the river
425 runoff (station A-E, L-O in Figs. 6, 8 and 16). The river nutrient loading used in this study is based
426 on mainly the HBV model output. Due to lack of observations, a detailed validation of river loading
427 may not be feasible. Moreover, only big rivers are included. Recent study found that small rivers
428 may have a significant contribution to the total river nutrient loading to the Baltic Sea
429 (unpublished). For ecological modeling, including nutrient loads from smaller rivers will improve
430 not only the total amount of nutrient inputs to the Baltic Sea but also the locations of the riverine
431 nutrient sources.

432 Some impacts from improper initial conditions may last for quite a long period, even for the whole
433 simulation duration, especially in deep areas and near bottom. For example, the large initial errors
434 for bottom DIN and DO at stations G, J, K last for quite a long period (Fig. 7 and 12). The
435 comparison between vertical profiles of model results and those of observations reflects obvious
436 differences for DIN and DO at the beginning of simulation. The initial model errors only decay
437 slowly (Fig 13c, f, i, l). The strong permanent stratification of salinity of observations is located at
438 the depth of 60 m, while the corresponding stratification of model results is at the depth of 80 m,
439 none of them even changes at all during two years of simulation (Fig. 13b, h). This might reflect
440 that insufficient vertical mixing slows down the initial errors decaying.

441 4.3 Assessment schemes

442 Statistical measures and point-to-point comparison are the common schemes to assess model skills
443 (Lacroix et al., 2007; Lewis and Allen, 2009; Ruzicka, 2011). Statistical measures can use all
444 available data and avoid subjective involvement in selecting observed data. However, there are two
445 caveats that we must be aware of. First, statistical measures cannot ensure a proper representation
446 for each observed data. For example, the statistical measures show the model-observation fit is
447 rather poor for DIN in surface (Table 2), however, the point-to-point comparison shows that model
448 results can reflect the basic seasonal variability (Fig. 6). This inconsistency is caused by extreme
449 outliers in data set, like the data from estuaries. In some other cases, equal representation of each
450 data is not reasonable. For example, two observations respectively from densely and sparsely
451 sampled areas (in time or space) should not equally contribute to the spatial mean. Second,
452 statistical measures are usually used to show the overall model skill, rather than describe model
453 skills along different dimensions. The point-to-point comparison is very effective to analyze the
454 model performance at the selected station, especially to evaluate model robustness to reproduce a
455 certain dynamic process, provided time-series of observed data. The shortcoming of the point-to-
456 point comparison includes the following four aspects. First, the point-to-point comparison has a
457 limited representation, as the ecological properties can differ a lot in various sub-regions. Second,
458 the point-to-point comparison is limited to the stations with time-series of data, but other data, e.g.
459 those from cruises will not be used. Third, it is inevitable to have subjective involvement in
460 selecting stations and layers, which is necessary for model developer's sake of good representation
461 to analyze model performance, but not appreciable for users/customers who are interested in an
462 objective assessment of the quality of the operational products. Finally, it is inconvenient to
463 implement a point-to-point comparison at too many stations.

464 The comprehensive comparison scheme (Wan et al., 2011) uses all available observations in the
465 entire model domain. This scheme deploys a grid in the spatial-temporal domain to properly

466 distribute data representations. The gridded data from all resources makes it possible to analyze the
467 model skills along different dimensions (Fig. 14, 15, 16). There is no subjective involvement in
468 selecting data. Thus, the comprehensive validation scheme can provide a relatively rigorous and
469 throughout assessment of model skills along different dimensions. However, the comprehensive
470 validation scheme will only be effective for systems with abundant observations. Thus, the
471 comprehensive validation cannot replace the point-to-point comparison. It is important to deploy
472 the traditional point-to-point comparison and statistical measures along with the comprehensive
473 validation in order to assess model skills quantitatively.

474 5. Summary

475 Following the inter-comparison experiments of the MyOcean project, the model system with the
476 latest feature (Wan et al., 2012) is assessed for its skills in providing biogeochemical information
477 service. The abundant observation data in the Baltic Sea allow us to implement a comprehensive
478 model validation scheme, which makes use of all available observation data to assess model skills
479 along each dimension. The comprehensive model validation scheme combined with the traditional
480 point-to-point comparison and statistical measures makes it possible to provide a relatively rigorous
481 assessment of model skills and to identify the major model errors and the main causes behind.

482 According to criteria used in the Baltic Sea and nearby regions (Maréchal, 2004; Radach and Moll,
483 2006), model skills for temperature, salinity, DIP and DO is scored either “excellent” or “very
484 good”. The model skill for Chl *a* is only scored “very good” on the PB criterion, but “poor”
485 according to both CF and ME criteria. The model skill for DIN would be scored “good” on the PB
486 criterion, “reasonable” on the CF criterion, but “poor” according to the ME criterion.

487 This assessment reflects that the model errors are mainly caused by insufficient light penetration,
488 excessive organic particle export downward, insufficient regional adaptation and uncertainties in
489 riverine nutrient loading, physical forcing and initial fields. This study highlights the importance to
490 apply multiple schemes (the comprehensive validation scheme, the point-to-point comparison and

491 the statistical measures) in order to assess model skills rigidly and to identify main causes for major
492 model errors effectively.

493

494 Acknowledgements

495 We would like to thank Per Berg for technical assistance with the HBM model code and setups, and
496 to thank the Swedish Meteorological and Hydrological Institute and the Bundesamt für
497 Seeschiffahrt und Hydrographie in Hamburg, Germany for providing the river data. This work was
498 supported by European Commission FP6 and FP7 projects ECOOP (Contract No. 036355),
499 MYCOEAN (Contract No. 218812) and MEECE (Contract No. DK18159104).

500 References

- 501 Allen, J. I., Holt, T. J., Blackford, J., and Proctor, R.: Error quantification of a high-
502 resolution coupled hydrodynamic-ecosystem coastal-ocean model: Part 2. Chlorophyll-a,
503 nutrients and SPM, *J. Marine Syst.*, 68, 381–404, 2007.
- 504 Almroth, E. and Skogen, M.D.: A North Sea and Baltic Sea model ensemble eutrophication
505 assessment, *Ambio*. 39, 59-69, 2010.
- 506 Berg, P. and Poulsen, J. W.: Implementation details for HBM. DMI Technical Report No.
507 12-11, ISSN: 1399-1388, Copenhagen, 2012.
- 508 Bergström, S.: Development and application of a conceptual runoff model for Scandinavian
509 catchments, Ph.D. thesis., SMHI Reports RHO, No. 7, Norrköping, 1976.
- 510 Bergström, S.: The HBV model – its structure and applications, SMHI Reports RH, No. 4,
511 Norrköping, 1992.
- 512 Conkright, M. E., Locarnini, R., Garcia, H., O’Brien, T., Boyer, T. P., Stephens, C., and
513 Antonov, J.: World ocean atlas 2001, objective analyses, data statistics and figures, CDROM
514 documentation, National Oceanographic Data Center, Silver Spring, MD, 2002.
- 515 Edelvang, K., Kaas, H., Erichsen, A. C., Alvarez-Berastegui, D., Bundgaard, K., and
516 Jørgensen, P. V.: Numerical modeling of phytoplankton biomass in coastal waters, *J. Marine*
517 *Sys.*, 57, 13–29, 2005.
- 518 Eilola, K., Meier, H. E. M., and Almroth, E.: On the dynamics of oxygen, phosphorus and

519 cyanobacteria in the Baltic Sea: a model study, *J. Marine Sys.*, 75, 163–184, 2009.

520 Fennel, W.: Model of the yearly cycle of nutrients and plankton in the Baltic Sea, *J. Mar.*
521 *Syst.* 6, 313-329, 1995.

522 Fennel, W. and Neumann, T.: The mesoscale variability of nutrients and plankton as seen in
523 a coupled model, *Ger. J. Hydrogr.* 48, 49-71, 1996.

524 Fennel, W. and Neumann, T.: Variability of copepods as seen in a coupled physical
525 biological model of the Baltic Sea, *ICES Marine Science Symposia* 219, 208-219, 2003.

526 Janssen, F., Neumann, T., and Schmidt, M.: Inter-annual variability in cyanobacteria blooms
527 in the Baltic Sea controlled by wintertime hydrographic conditions, *Mar. Ecol. Prog. Ser.*
528 275, 59-68, 2004.

529 Kuznetsov, I., Neumann, T., and Burchard, H.: Model study on the ecosystem effect of a
530 variable C:N/ P ratio for cyanobacteria in the Baltic Proper, *Ecol. Model.*, 219, 107–114,
531 2008.

532 Lacroix, G., Ruddick, K., Park, Y., Gypens, N., and Lancelot, C.: Validation of the 3D
533 biogeochemical model MIRO&CO with field nutrient and phytoplankton data and MERIS-
534 derived surface chlorophyll images, *J. Mar. Syst.* 64, 66-88, 2007.

535 Langner, J., Andersson, C., and Engardt, M.: Atmospheric input of nitrogen to the Baltic Sea
536 basin: present situation, variability due to meteorology and effect of climate change, *Boreal*
537 *Environ. Res.*, 14, 226–237, 2009.

538 Lewis, K. and Allen, J. I.: Validation of a hydrodynamic-ecosystem model simulation with
539 time-series data collected in the western English Channel, *J. Marine Syst.*, 77, 296–311,
540 2009.

541 Maar, M., Møller, E. F., Larsen, J., Kristine, S. M., Wan. Z., She, J., Jonasson, L., and
542 Neumann, T.: Ecosystem modeling across a salinity gradient from the North Sea to the Baltic
543 Sea, *Ecol. Model.*, 222, 1696–1711, 2011.

544 Maréchal, D.: A Soil-Based Approach to Rainfall-Runoff Modelling in Ungauged
545 Catchments for England and Wales, PhD Thesis, Cranfield University. 157 pp, 2004.

546 Neumann, T.: Towards a 3D-ecosystem model of the Baltic Sea, *J. Marine Sys.*, 25, 405–
547 419, 2000.

548 Neumann, T.: The fate of river-borne nitrogen in the Baltic Sea: An example for the River
549 Oder. *Estuar., Coast. and Shelf S.* 73, 1-7, 2007.

550 Neumann, T., Fennel, W., and Kremp, C.: Experimental simulations with an ecosystem
551 model of the Baltic Sea: a nutrient load reduction experiment, *Global Biogeochem. Cy.*, 16,
552 7(1)–7(19), 2002.

553 Neumann, T., Schernewski, G.: An ecological model assessment of two nutrient abatement
554 strategies for the Baltic Sea, *J. Mar. Syst.* 56, 195-206, 2005.

555 Neumann, T. and Schernewski, G.: Eutrophication in the Baltic Sea and shifts in nitrogen
556 fixation analyzed with a 3-D ecosystem model, *J. Marine Sys.*, 74, 592–602, 2008.

557 OSPAR, Villars, M., Vries, I.D., Bokhorst, M., Ferreira, J., Gellers-Barkman, S., Kelly-
558 Gerreyn, B., Lancelot, C., Ménesguen, A., Moll, A., Pätsch, J., Radach, G., Skogen, M.,
559 Soiland, H., Svendsen, E., Vested, H.J., 1998. Report of the ASMO modeling workshop on
560 eutrophication issues, 5-8 November 1996. The Hague, The Netherlands. OSPAR
561 Commission Report, RIKZ, The Hague: 102.

562 Radach, G. and Moll, A.: Review of the Three-Dimensional Ecological Modelling Related to

563 the North Sea Shelf System – part 2: Model Validation and Data Needs. *Oceanography and*
564 *Marine Biology – an Annual Review*, vol. 44, pp. 1-60, 2006.

565 Ruzicka, J.J., Wainwright, T.C., and Peterson, W.T.: A simple plankton model for the
566 Oregon upwelling ecosystem: Sensitivity and validation against time-series ocean data,
567 *Ecological Modelling*, 222 (6), 1222-1235, 2011.

568 Rykiel, E.J., Jr.: Testing ecological models: the meaning of validation, *Ecol. model.* 90, 229-
569 244, 1996.

570 Savchuk, O. P., Wulff, F., Hille, S., Humborg, C., and Pollehne, F.: The Baltic Sea a century
571 ago – a reconstruction from model simulations, verified by observations, *J. Marine Sys.*, 74,
572 485–494, 2008.

573 She, J., Berg, P., and Berg, J.: Bathymetry effects on water exchange modeling through the
574 Danish Straits, *J. Marine Sys.*, 65, 450– 459, 2007a.

575 She, J., Høyer, J., and Larsen, J.: Assessment of sea surface temperature observational
576 networks in the Baltic Sea and North Sea, *J. Marine Sys.*, 65, 314–335, 2007b.

577 Stigebrandt, A. and Wulff, F.: A model for the dynamics of nutrients and oxygen in the
578 Baltic proper, *J. Mar. Res.* 45, 729-759, 1987.

579 Tian, T., Merico, a., Su J., Staneva, J., Wiltshire, K., and Wirtz, K.: Importance of
580 resuspended sediment dynamics for the phytoplankton spring bloom in a coastal marine
581 ecosystem, *J. Sea Res.*, 62, 214–228, 2009.

582 Wan, Z., Jonasson, L., and Bi, H.: N/ P ratio of nutrient uptake in the Baltic Sea, *Ocean Sci.*,
583 7, 693–704, 2011.

584 Wan, Z., Bi, H., She, J., Maar, M., and Jonasson, L.: Model study on horizontal variability of
585 nutrient N/P ratio in the Baltic Sea and its impacts on primary production, nitrogen fixation
586 and nutrient limitation, *Ocean Sci. Discuss.*, 9, 385-419, doi:10.5194/osd-9-385-2012, 2012.

587

588 Figure legends

589 Fig. 1 Topography of the Baltic Sea (unit: m) and location of time-series observational
590 stations A-R (marked with *).

591

592 Fig. 2 Seasonal variability of temperature in surface layer

593 Red solid curve (black dashed cycles) for model results (observations). Unit: °C. Panels A-R
594 for Stations A-R (Fig. 1), respectively.

595

596 Fig. 3 Seasonal variability of temperature in bottom layer

597 Notations same as in Fig. 2.

598

599 Fig. 4 Seasonal variability of salinity in surface layer

600 Red solid curve (black dashed cycles) for model results (observations). Unit: PSU. Panels A-
601 R for Stations A-R (Fig. 1), respectively.

602

603 Fig. 5 Seasonal variability of salinity in bottom layer

604 Notations same as in Fig. 4.

605

606 Fig. 6 Seasonal variability of DIN in surface layer

607 Red solid curve (black dashed cycles) for model results (observations). Unit: mmol m^{-3} .

608 Panels A-R for Stations A-R (Fig. 1), respectively.

609

610 Fig. 7 Seasonal variability of DIN in bottom layer

611 Notations same as in Fig. 6.

612

613 Fig. 8 Seasonal variability of DIP in surface layer

614 Notations same as in Fig. 6.

615

616 Fig. 9 Seasonal variability of DIP in bottom layer

617 Notations same as in Fig. 6.

618

619 Fig. 10 Seasonal variability of Chl *a* in surface layer

620 Red solid curve (black dashed cycles) for model results (observations). Unit: mg m^{-3} . Panels

621 A-R for Stations A-R (Fig. 1), respectively.

622

623 Fig. 11 Seasonal variability of DO in surface layer

624 Notations same as in Fig. 6.

625

626 Fig. 12 Seasonal variability of DO in bottom layer

627 Notations same as in Fig. 6.

628

629 Fig. 13 Temporal evolutions of vertical profile in the Gotland deep at station I

630 Panels A-F for observations of temperature, salinity, DIN, DIP, Chl *a*, DO, respectively;

631 Panels G-R for model results of them. Units: temperature -- °C; Chl *a* – mg m⁻³; DIN, DIP,

632 DO – mmol m⁻³.

633

634 Fig. 14 Overall pattern of seasonal variability

635 Red solid curve (black dashed cycles) for model results (observations). Panels A-F for,

636 temperature, Chl *a*, DIP, salinity, DIN, DO, respectively. Units same as in Fig. 13.

637

638 Fig. 15 Overall pattern of vertical profile

639 Notations same as in Fig. 14.

640

641 Fig. 16 Horizontal pattern of model's percentage errors

642 Panels A-F for, temperature, Chl *a*, DIP, salinity, DIN, DO, respectively. Units %.

643

644 Fig. 17 Inter-comparison among modeled, satellite detected and in-situ observed Chl *a* in
645 surface layer

646 Blue solid curve for satellite detected results. Other notations same as in Fig. 10.

647

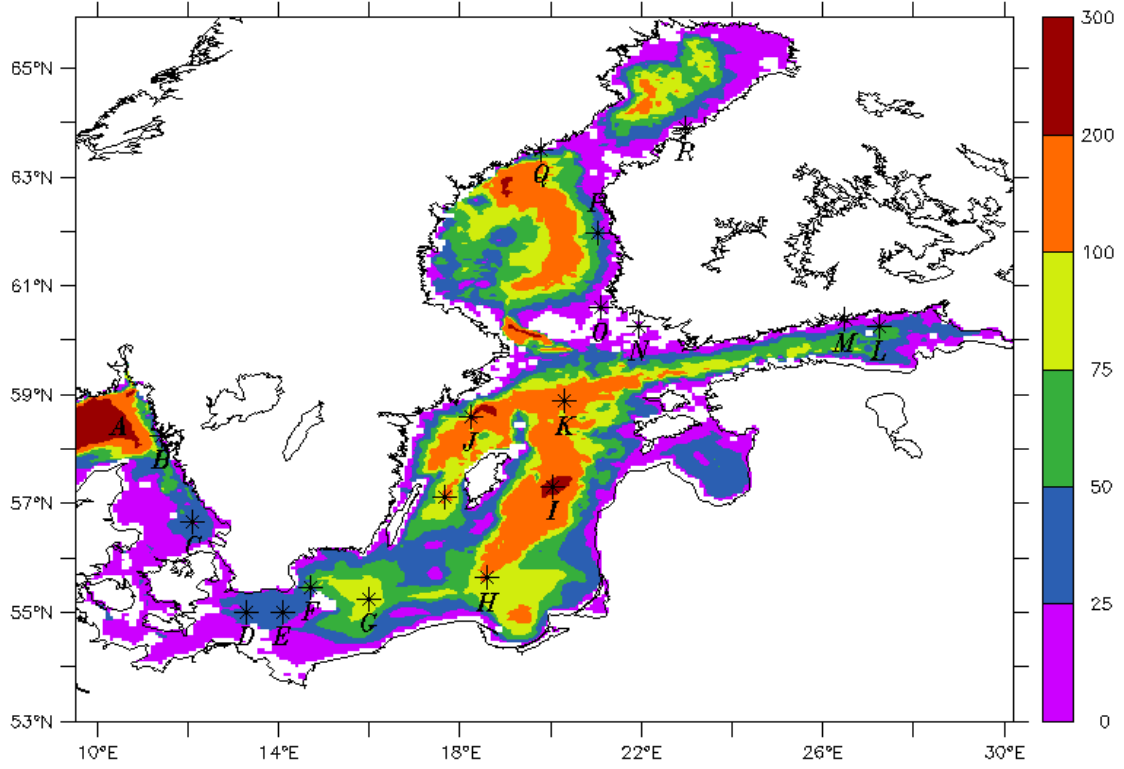


Fig. 2

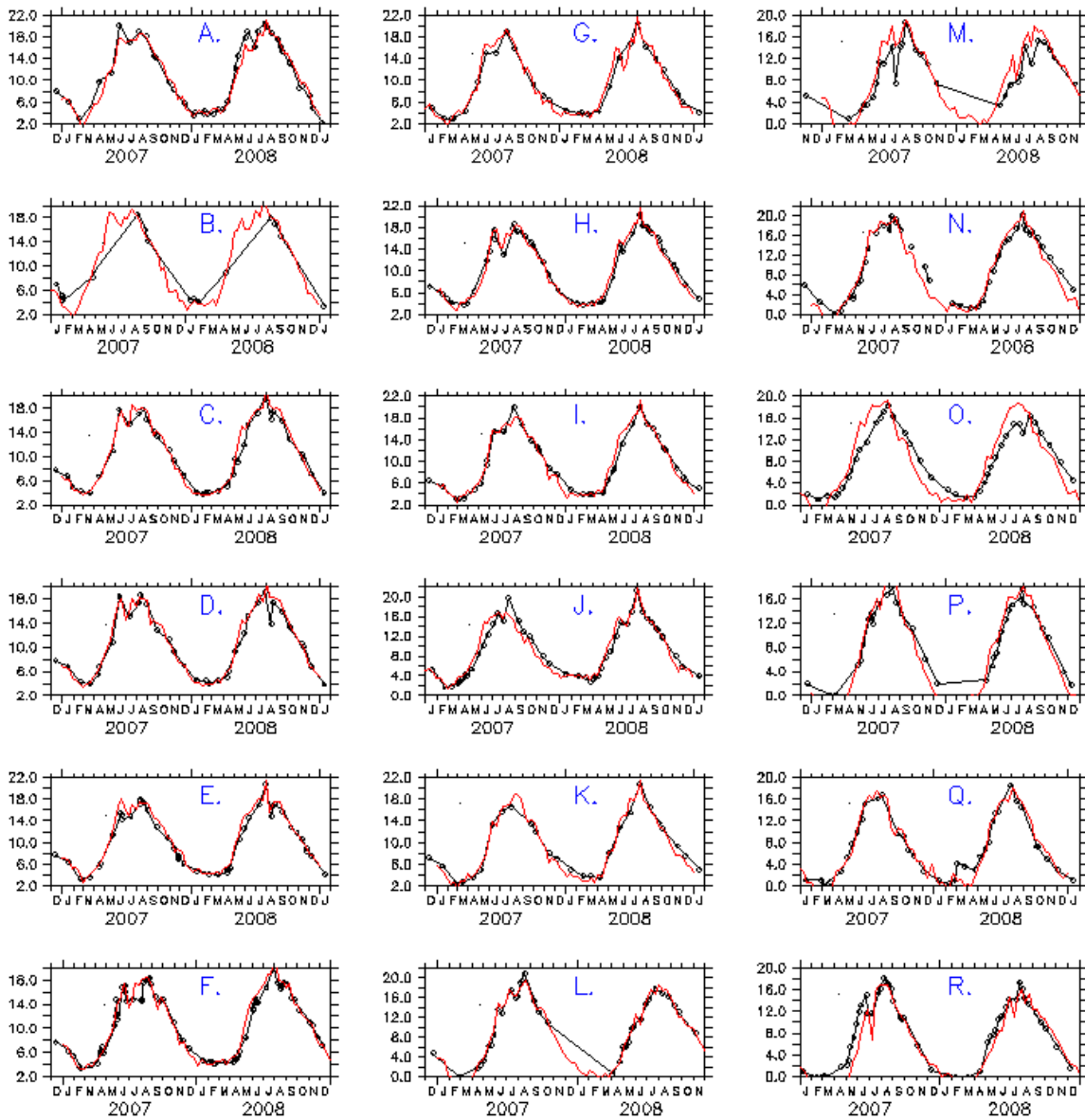


Fig. 3

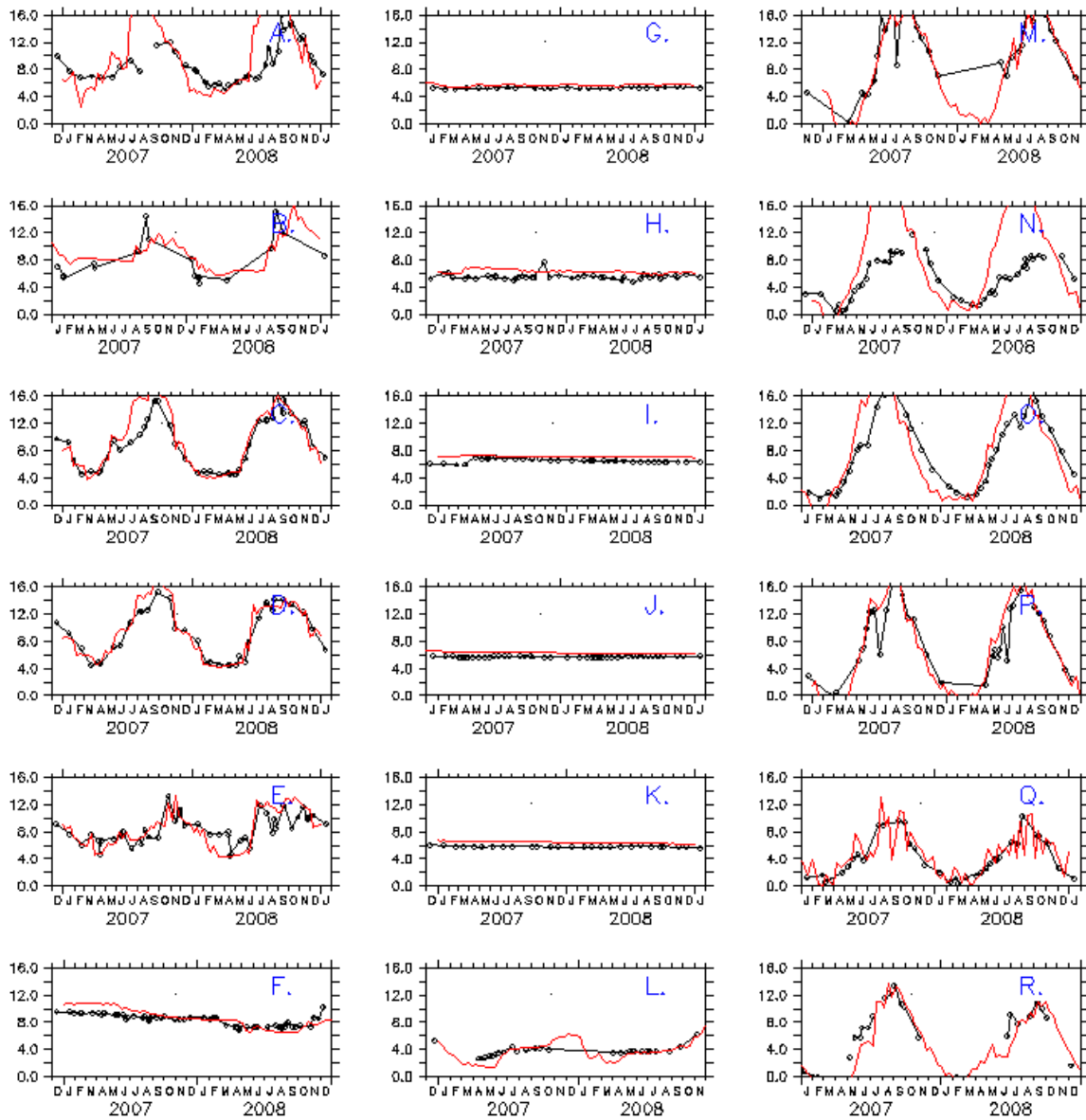


Fig. 4

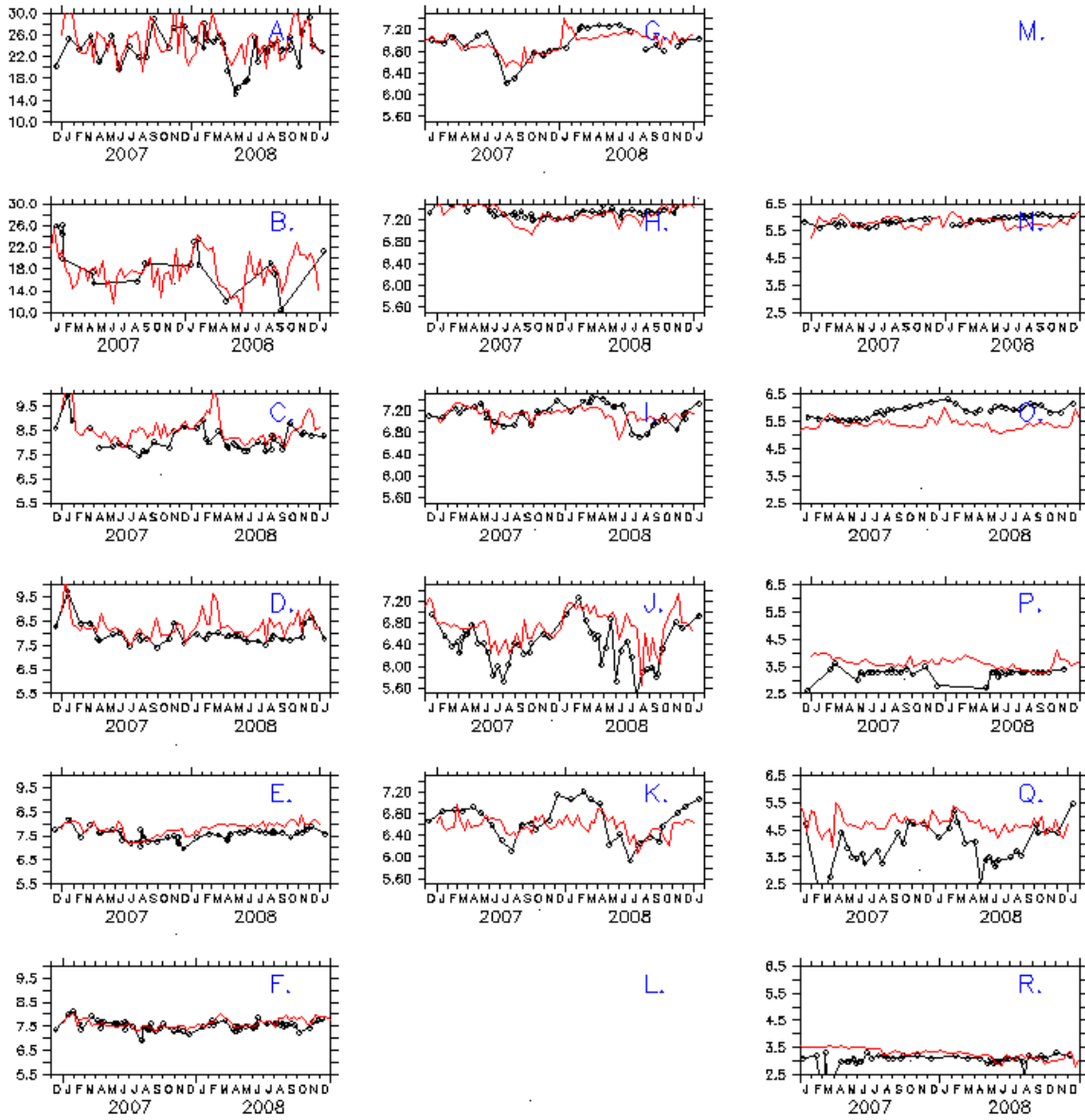


Fig. 5

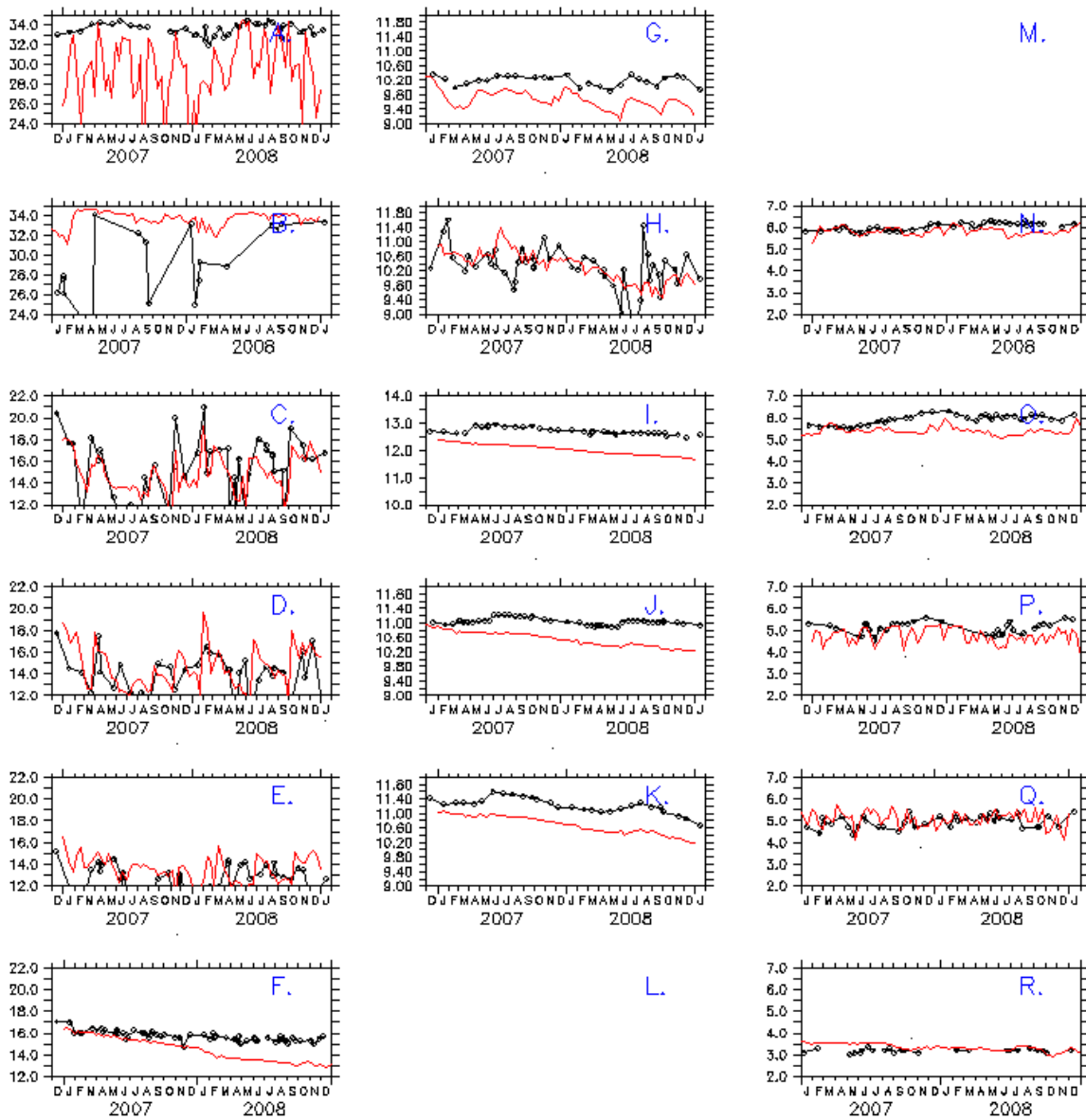


Fig. 6

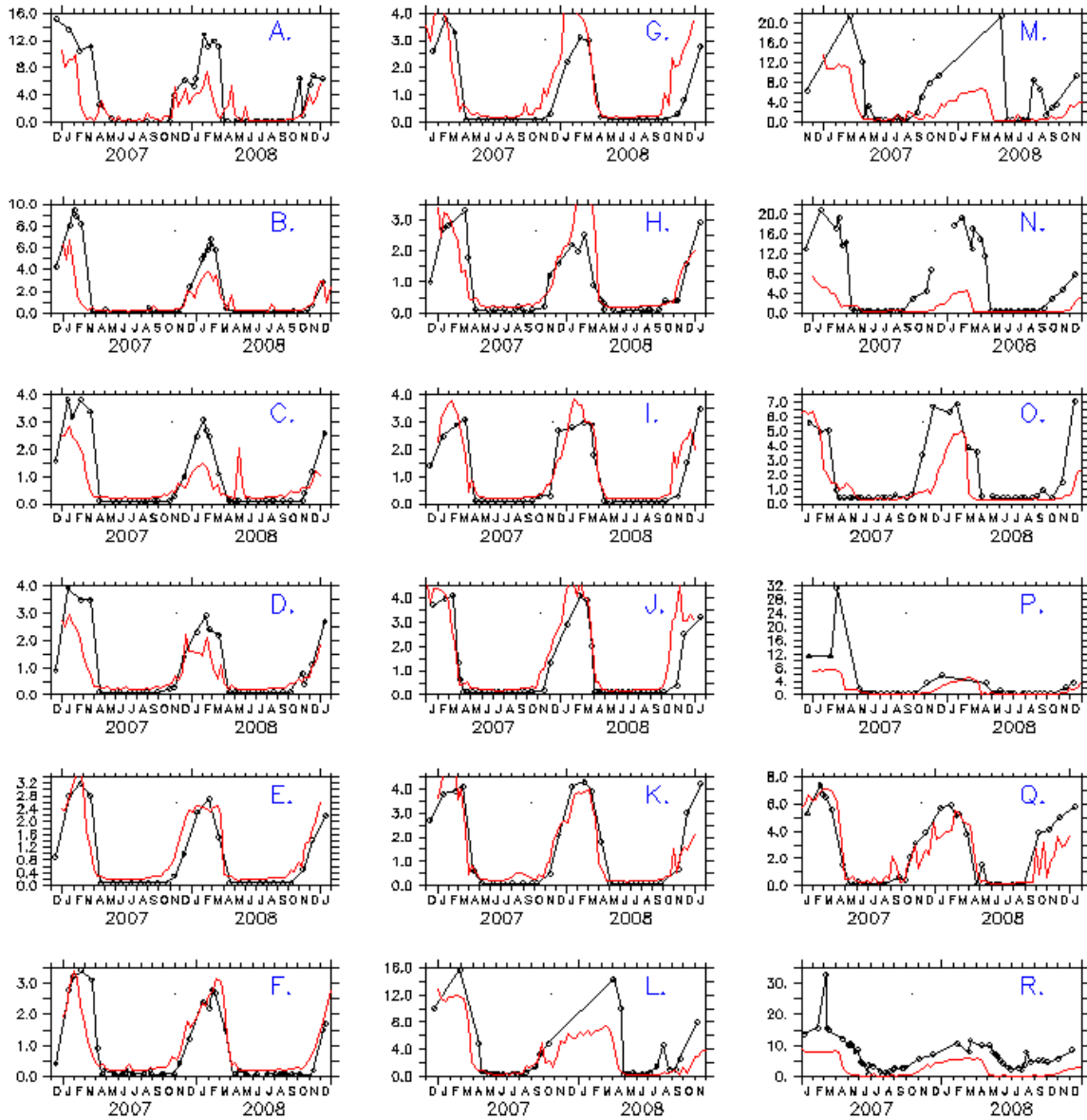


Fig. 7

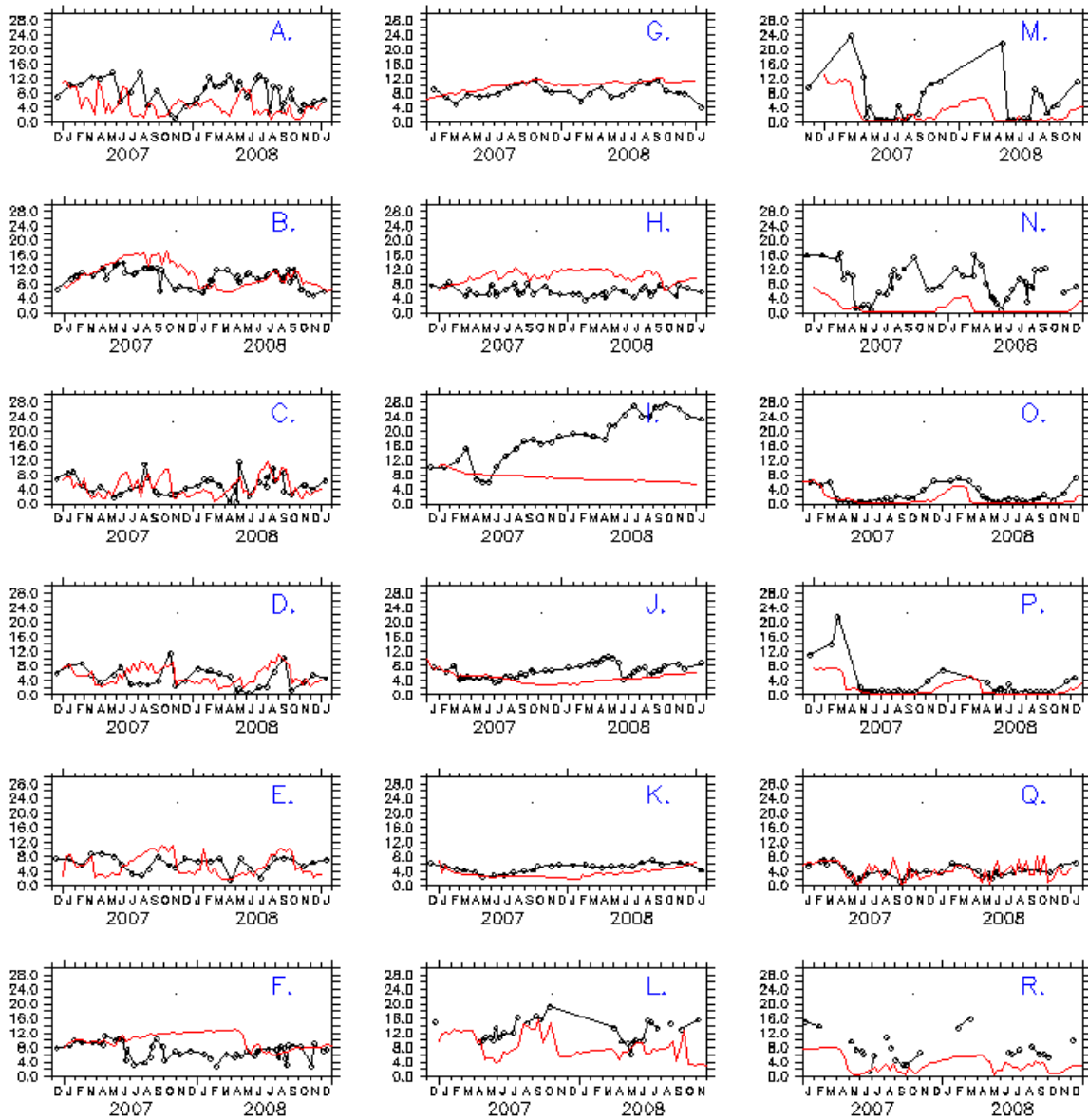


Fig. 8

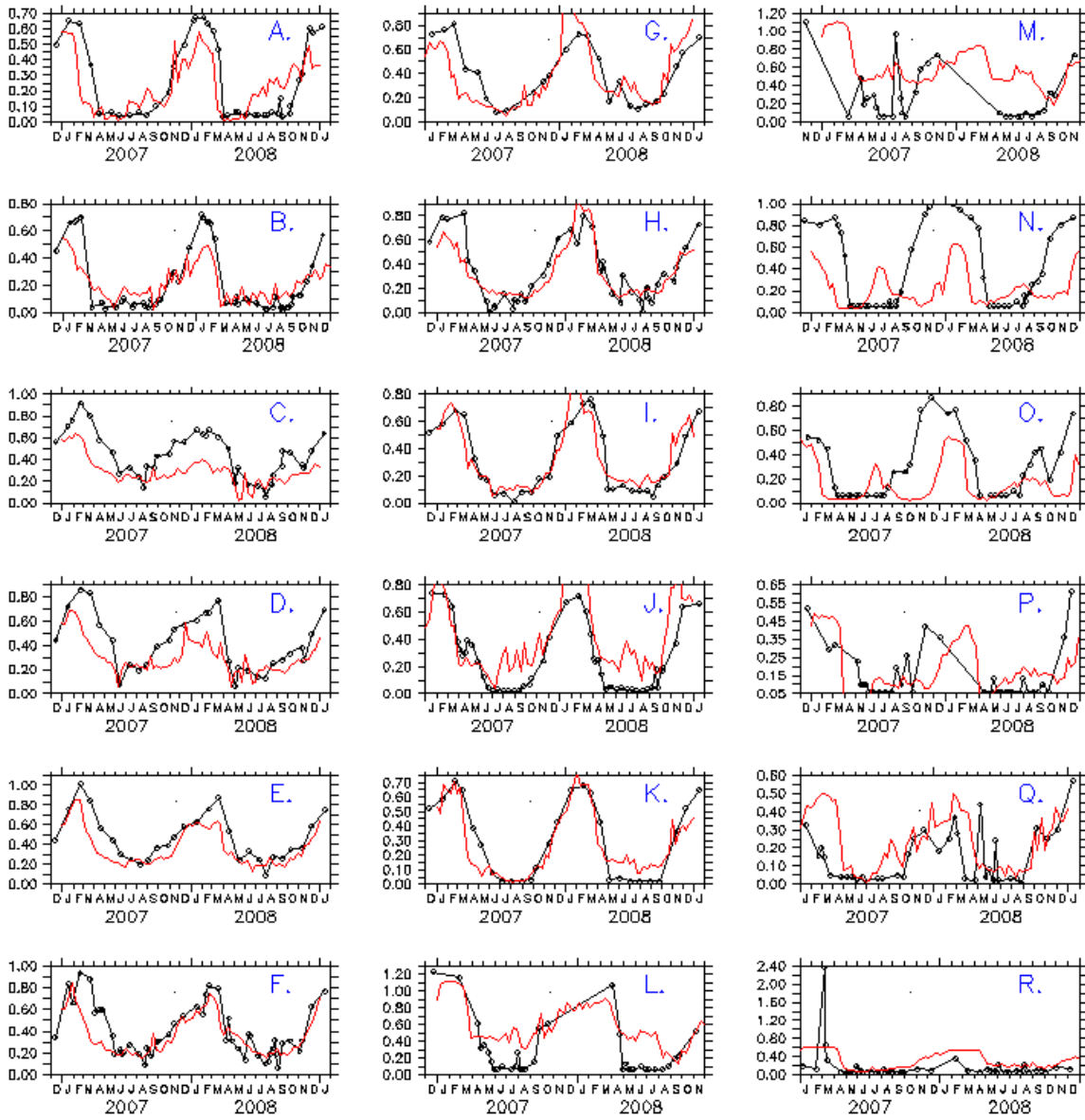


Fig. 9

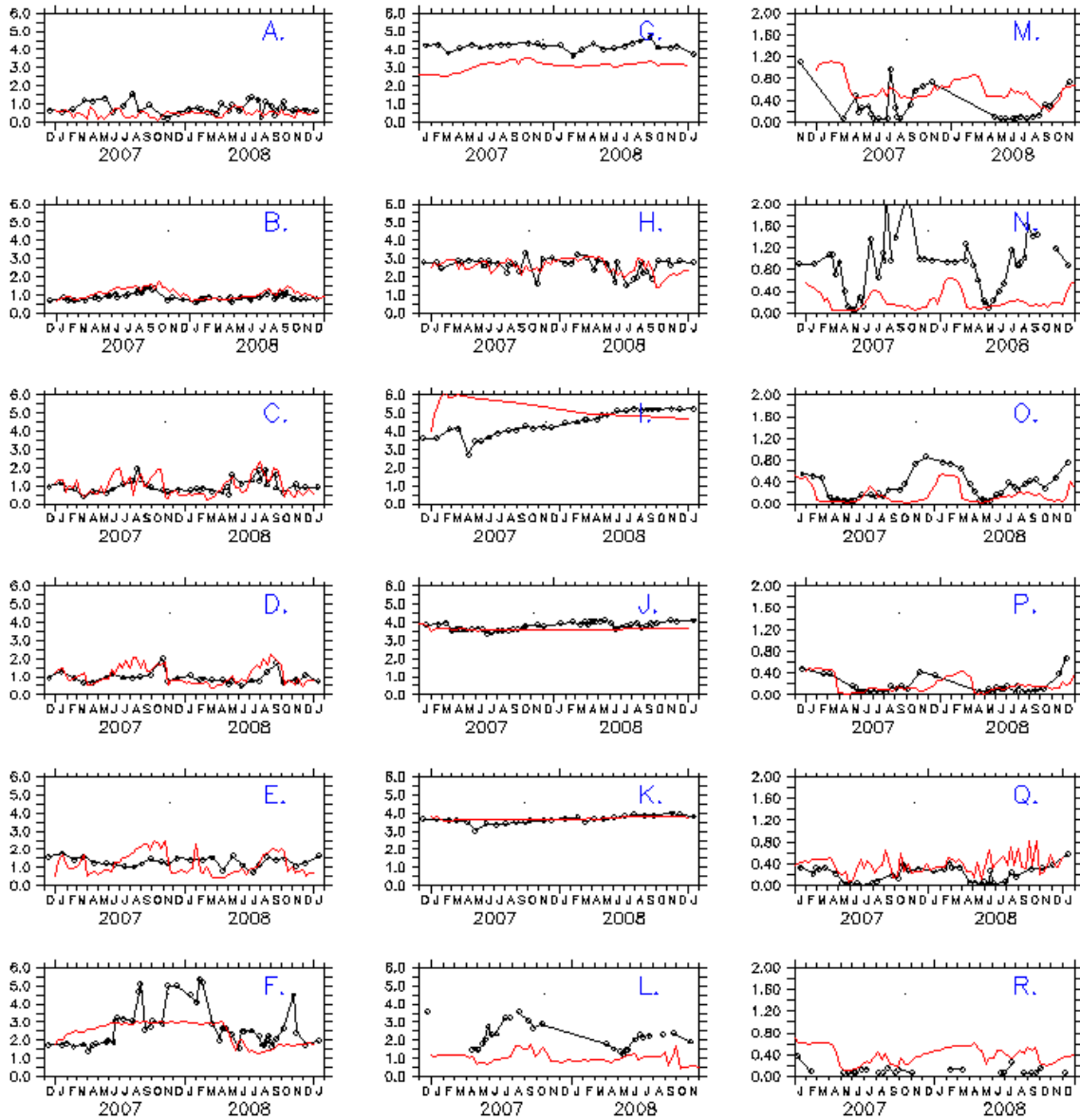


Fig. 10

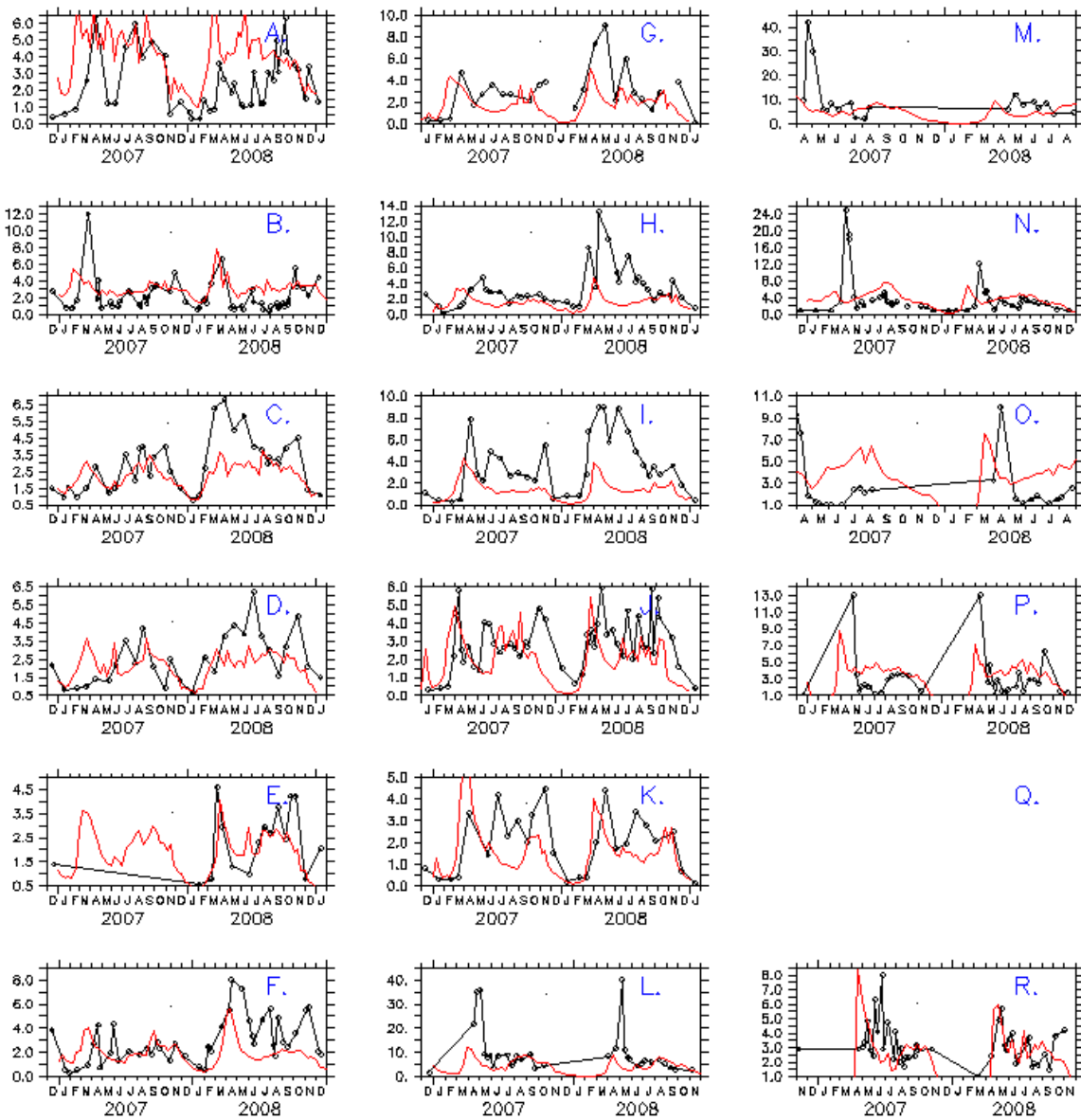


Fig. 11

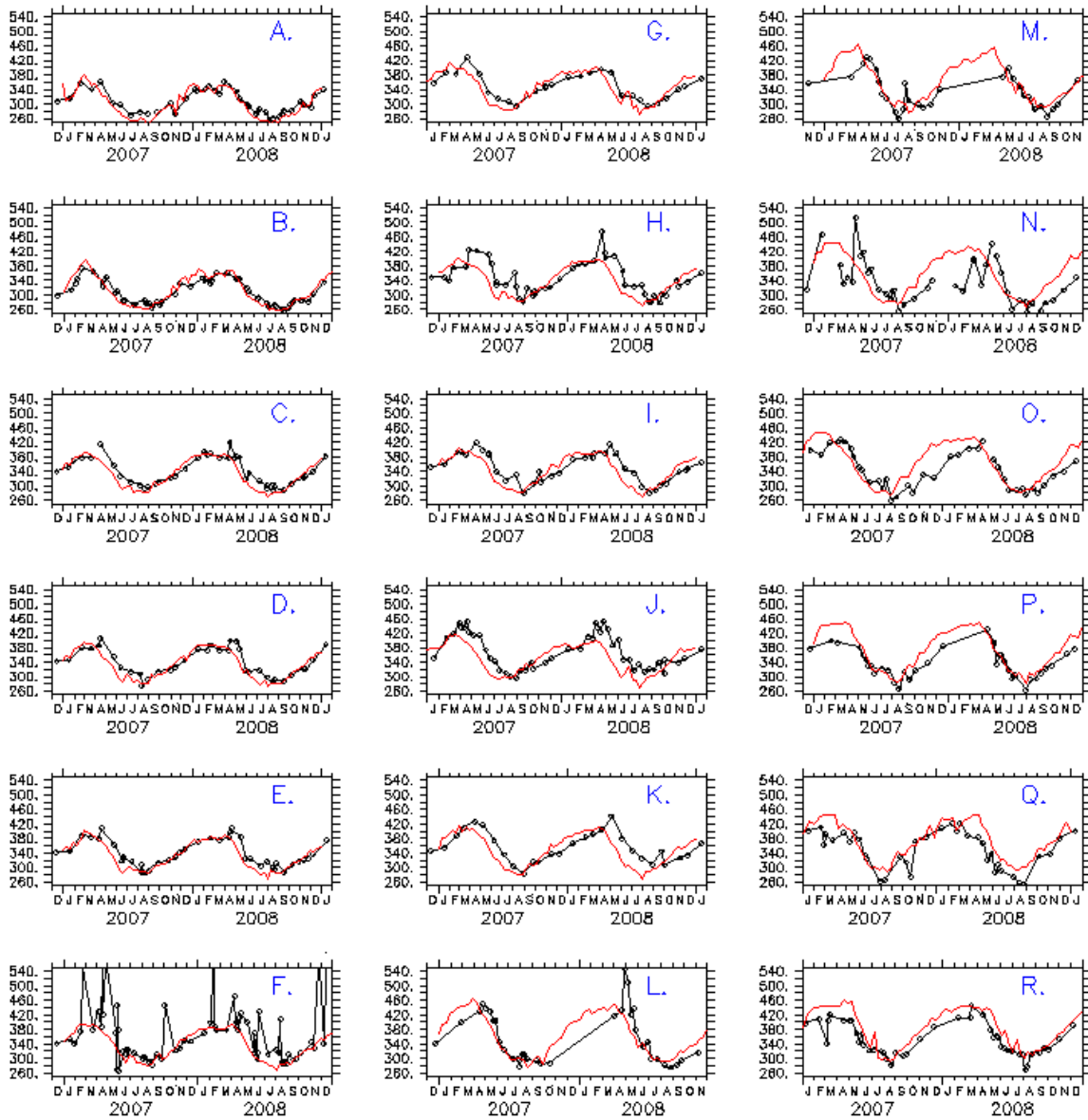


Fig. 12

